5th Joint International Symposium on Deformation Monitoring (JISDM), 20-22 June 2022, Valencia, Spain
DOI: http://doi.org/10.4995/JISDM2022.2022.13869

PS-InSAR and UAV technology used in the stability study of Ankang expansive soil airport

Jinzhao Si[1], Shuangcheng Zhang[1], Yufen Niu[2]

[1] College of Geology Engineering and Geomatics, Chang'an University, Xi'an 710054, China, (SiJinzhao_chd@163.com; shuangcheng369@chd.edu.cn)
[2] College of Mining and Geomatics Engineering, Hebei University of Engineering, Handan 056038, China, (niuyufenpippa@163.com)

Key words: *PS-InSAR; corner reflectors; expansive soil; UAV measurement; stability analysis; Ankang airport*

ABSTRACT

Expansive soil is a natural geological body with obvious expansion and contraction, multiple fissures and other undesirable properties. The deformation monitoring of expansive soil in high-fill areas under the combined action of wet expansion and dry contraction has become a hotspot of related research. to large-scale soil disasters. Time-series Interferometric Synthetic Aperture Radar (InSAR) technology is widely used in the monitoring of various geological hazards due to its advantages of wide coverage, high monitoring accuracy, and all-weather operation. This study takes Ankang Airport (AKA) expansive soil airport as an example. First, the ground digital elevation model (DEM) of the airport filling area was obtained by using UAV; secondly, the deformation rate and deformation time series of the expansive soil airport were obtained by using the persistent scatterer InSAR (PS-InSAR) technology; third, for the coherence In poor areas, artificial corner reflectors (CR) are arranged to increase stable scattering points; Finally, the deformation time series of feature points are extracted, combined with regional precipitation data analysis, the relationship between the periodic deformation of the airport expansive soil slope and rainfall. There is a subsidence trend along the LOS direction in the dry season, which is consistent with the expansion and contraction characteristics of expansive soils. Finally, the deformation rate is proportional to the depth of the expansive soil fill. It is judged that the existing small surface deformation and its periodic deformation distribution are caused by the combined action of the settlement after construction of the expansive soil filling area and the expansion and contraction characteristics of the expansive soil.

I. INTRODUCTION

Ankang Airport (AKA) started construction in 2016, and the airport was completed in May 2020. This airport is located in the Ankang Yuehe Basin at the southern of the Qinling Mountains in China. The Expansive soil is widely distributed in this area. Expansive soil is a naturally formed multi-fractured geological body, which has unfavourable properties such as significant expansion and shrinkage, over-consolidation and multi-fracture. In addition, the topographic drop at the original site of AKA is large, therefore during the construction of the airport, the filling volume has reached 30,000,000 m^3, and the vertical height difference has reached 94 m. To sum up, the consolidation and compression characteristics of large-scale fill soil and the special hydraulic characteristics of expansive soil have caused certain hidden dangers, threatening the safe navigation of AKA at all times. Therefore, it is very necessary to conduct real-time monitoring and stability analysis of AKA.

The widely applied methods for the airport surface deformation include global navigation satellite system (GNSS) measurement and levelling measurement. However, these methods have high cost of manual equipment and can only obtain relatively discrete point deformation data, making it difficult to monitor the overall deformation of the study area. InSAR (synthetic aperture radar interferometry) technology, as a new type of earth observation method, can overcome the shortcomings of traditional observation methods. Through the two kinds of observation values of intensity and phase, InSAR technology can obtain high-resolution surface deformation information, and realize large-scale spatial detection and long-period precision monitoring (Berardino *et al.*, 2002). Recently, time-series InSAR technology has been widely used in various airports for long-term deformation monitoring and mechanism analysis, such as China Shanghai Pudong Airport (Jiang *et al.*, 2016), Xiamen Xiang'an Airport (Zhuo *et al.*, 2020; Liu *et al.*, 2019) and Hong Kong Chek Lap Kok Airport (Wu *et al.*, 2020; Jiang and Lin, 2010), and Kuala Lumpur International Airport in Malaysia (Jiang *et al.*, 2016) where the special properties of tropical peat cause subsidence. In addition, InSAR technology is also applied to some mountainous airports with similar geological conditions to Ankang Airport, such as Iqaluit Airport in Canada (Short *et al.*, 2014), and Yan'an New Airport in China (Wu *et al.*, 2019).

In recent years, the characteristics of time series InSAR technology have also been proved to be suitable for monitoring Periodic slow deformation caused by special hydraulic properties of expansive soil (Gabriel et al., 1989). In this paper, we attempt to identify and understand local subsidence activity in the AKA area by using MT-InSAR techniques. The dataset used in this paper consists of 26 Sentinel-1A scenes, with a time span from May 2020 to June 2021. First, considering the migration of a large amount of surface material in the AKA will cause the historical DEM products to be unable to remove the topographic phase effectively, we choose the UAV to obtain the high-precision DEM of the AKA. In addition, in order to avoid the inability to obtain sufficiently stable scattering points, we arrange artificial corner reflectors in the de-coherence region according to the spatiotemporal distribution of coherence; secondly, the PS-InSAR method is used to monitor the surface deformation of AKA; finally, the deformation time of the feature points is extracted sequence, combined with regional geological and hydrological data, to analyse deformation inducement and stability.

II. Study Area and Datasets

Ankang Airport is located in the Ankang, Shanxi, China, as shown in Figure 1, which is about 15 km to the city center of the Ankang. The terminal area of AKA is 5,500 m^2; the runway is 2,600 m long and 45 m wide, which can meet the annual passenger needs. Demand for a throughput of 300,000 passengers and a cargo and mail throughput of 750 tons. AKA is located in the platform area on the northern margin of the Yue he Basin. There are a lot of expansive soils in this area, including clay, silty clay, gravel-like soil, sandstone, mudstone and conglomerate. The special hydraulic action of expansive soil is the fundamental cause of the instability of expansive soil, which mainly includes the effects of expansion and contraction deformation, crack development and strength reduction caused by changes in moisture and stress. These characteristics can easily cause potential geological hazards to the infrastructure on the soil.

Considering the large degree of excavation and filling in the airport and the drastic historical changes of the ground surface, external DEM products such as SRTM DEM and ASTER GDEM often cause serious DEM errors due to their poor timeliness. Therefore, a DEM with a regular grid spacing of 5 m and a vertical resolution of 2 m acquired by UAV was used to simulate and remove the terrain phase contribution during the generation of the interferogram, and from the range Doppler coordinates to those corresponding to the WGS84 coordinate system Geo-recoding, DEM products are shown in Figure 1b.

The monitoring experiment selects the SAR image data of 26 scenes in Interferometric Wide (IW) mode provided by Sentinel-1A satellite covering the study area from 2020-5 to 2021-7. The polarization mode is VV and VH dual polarization, the incident angle is 39.5°, and the resolution in the azimuth × range direction is 2.33 m × 13.99 m. The image data is as follows: track number 100, track configuration ASCENDING, and acquisition dates are May 2020. June 24; June 5, 17, 29; July 11, 23; August 4, 16, 28; September 21; October 3, 15, 27; November 8, 20; December 2, 26; January 7, 19, 31, 2021; February 12, 24; March 8, 20; March 8, 20; April 1, 13, 25; June 12; July 6. Detailed spatial and temporal baselines of these Sentinel-1 datasets are shown in Figure 2.

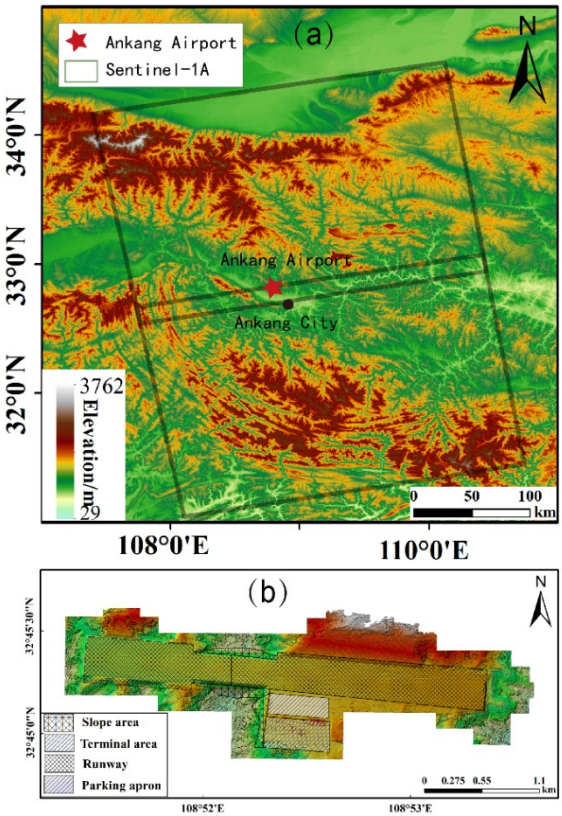

Figure 1. (a) Study area and data coverage; (b) DEM data and airport area division map.

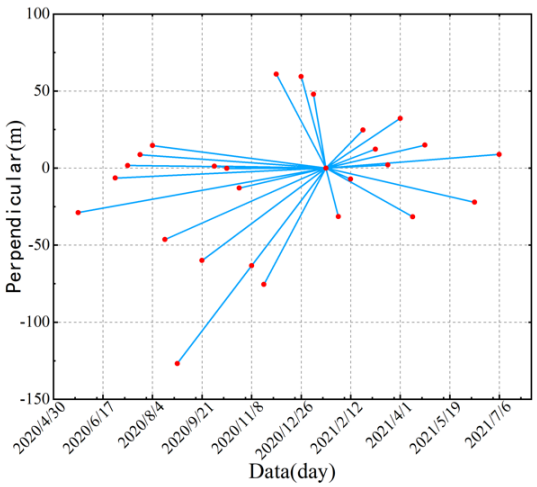

Figure 2. PS-InSAR Baseline Maps.

To restrain deformation, the airport operator planted low shrubs on the airport slopes and fill platforms. It is

well known that dense vegetation coverage tends to cause large changes in backscatter coefficients during repeated imaging, which can lead to regional de-coherence problems. (Touzi *et al.*, 1999).

As shown in Figure 3, We calculated the mean coherence of the selected interference pairs covering the study area. From the spatial distribution of the coherence coefficient, it can be clearly seen that there is an obvious de-coherence phenomenon in the filled slope, therefore we arrange artificial corner reflectors in this area to increase the stable scattering points in the de-coherent area.

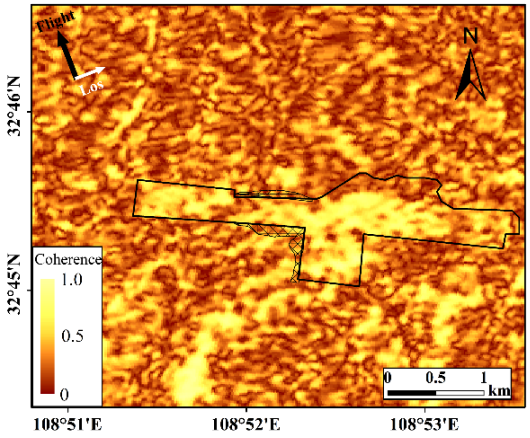

Figure 3. Coherence map.

The pictures of artificial corner are shown as Figure 4a and 4b. Figure 4c and 4d depicts the change of backscattering in the study area before and after the installation of the corner reflector. It can be seen from Figure 4 that after the corner reflector is installed, stable scattering points appear on the filled slope, which can increase the number of PS points and improve the InSAR monitoring accuracy.

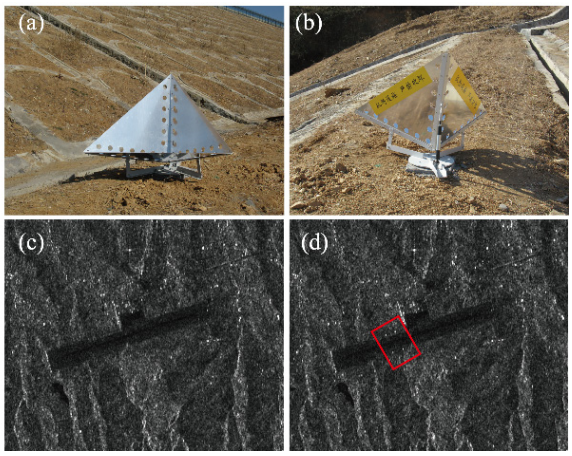

Figure 4. (a), (b) Site photo of artificial corner reflector; (c) backscattering map before the installation; (d) backscattering map after the installation.

III. DATA PROCESSING

The traditional differential interferometry technique is severely restricted in its application range due to the influence of time and space de-correlation and atmospheric delay. To solve these problems, the "Permanent Scatterers InSAR Technique" (PS-InSAR) has been proposed (Ferretti *et al.*, 2001). This technique utilizes the characteristic that the permanent scatterer (PS) can still maintain good coherence in a long period of time. Since PS-InSAR technology was proposed, related algorithms have also been developed one after another.

In this paper, the StaMPS approach proposed by Hooper (Hooper *et al.*, 2004.) is applied to process SAR data, and the corner reflectors are arranged in advance based on the interferometric pair coherence distribution to obtain enough PS points. The stamps approach selects the target with smaller amplitude dispersion and stable phase as the PS point, which can select a larger number of PS points than the conventional PS algorithm.

Assuming that there are N+1 SAR images in the study area, according to the perpendicular baseline, time baseline and Doppler frequency, a scene image is selected as the single main image, N interference pairs can be generated by interfering other images with this main image.

STAMPS approach is to form interferograms and remove most of the topographic phase signature using a digital elevation model (DEM). The residual phase: φ, of the x pixel in the i topographically corrected interferogram can be written as the sum of 5 terms (Eq. 1):

$$\varphi_{x,i} = \varphi_{def,x,i} + \varphi_{\alpha,x,i} + \varphi_{orb,x,i} + \varphi_{\varepsilon,x,i} + n_{x,i} \quad (1)$$

where φ_{def} = the phase change due to movement of the pixel in the satellite line-of-sight (LOS) direction
φ_{α} = the phase equivalent of the difference in atmospheric retardation between passes
φ_{orb} = the phase due to orbit inaccuracies
φ_{ε} = the residual topographic phase due to error in the DEM
n = the noise term due to variability in scattering from the pixel

We assume that that $\varphi_{def}, \varphi_{\alpha}, \varphi_{orb}$ are spatially correlated over a specified length, L, on the contrary, φ_{ε} and φ_{ε} are spatially uncorrelated over the same distance, with mean 0. If the positions of the other PS are known, averaging over all phases within a circular block of radius L centered at pixel x means that (Eq. 2):

$$\overline{\varphi}_{x,i} = \overline{\varphi}_{def,x,i} + \overline{\varphi}_{\alpha,x,i} + \overline{\varphi}_{orb,x,i} + \overline{\varphi}_{\varepsilon,x,i} + \overline{n}_{x,i} \quad (2)$$

where $\overline{\varphi}_{def}$ = the average of φ_{def}
$\overline{\varphi}_{\alpha}$ = the average of φ_{α}
$\overline{\varphi}_{orb}$ = the average of φ_{orb}

$\overline{\varphi}_{\varepsilon}$ = the average of φ_{ε}
$\overline{n}$ = the average of n

The small values of φ_{ε} and n can be ignored, subtracting Equation 2 from Equation 1 leaves (Eq. 3):

$$\varphi_{x,i} - \overline{\varphi}_{x,i} = \varphi_{\varepsilon,x,i} + n_{x,i} - \overline{n'}_{x,i} \quad (3)$$

where $\overline{n'}_{x,i} = n_{x,i} + \overline{\varphi}_{def,x,i} - \varphi_{def} + \overline{\varphi}_{\alpha} - \varphi_{\alpha} + \overline{\varphi}_{orb} - \varphi_{orb}$

The phase error from uncertainty in the DEM is proportional to the perpendicular component of the baseline (Fattahi and Amelung, 2013.) (Eq. 4):

$$\varphi_{\varepsilon,x,i} = B_{\perp,x,i} \cdot K_{\varepsilon,x} \quad (4)$$

where $B_{\perp,x,i}$ = the phase error from DEM
$K_{\varepsilon,x}$ = a proportionality constant

Equation 3 can be written as (Eq. 5):

$$\varphi_{x,i} - \overline{\varphi}_{x,i} = B_{\perp,x,i} \cdot K_{\varepsilon,x} + n_{x,i} - \overline{n'}_{x,i} \quad (5)$$

The phase stability evaluation method based on pixel time correlation is defined as (Eq. 6):

$$\gamma_x = \frac{1}{N}\left|\sum_{i=1}^{n} exp\left\{j(\varphi_{x,i} - \overline{\varphi}_{x,i} - \hat{\varphi}_{\varepsilon,x,i})\right\}\right| \quad (6)$$

where γ_x = the phase stability of the pixel
N = the number of available interferograms
$\hat{\varphi}_{\varepsilon,x,i}$ = the estimate of $\varphi_{\varepsilon,x,i}$

After the step of selecting PS based on the calculated values of γ_x in Equation 5, we estimate the DEM error and subtract it to get the corrected interferometric phase (Eq. 7):

$$\varphi_{x,i} - \Delta\hat{\varphi}_{\varepsilon,x,i} = \varphi_{def,x,i} + \varphi_{\alpha,x,i} + \varphi_{orb,x,i} + \varphi_{\varepsilon,x,i} + n_{x,i} \quad (7)$$

After unwrapping, four error terms remain in Equation 6 which is assumed to be uncorrelated temporally, we use some filters to remove these terms. The overall data processing flow is shown in Figure 5.

IV. Result and Analyse

We have applied the STAMPS technique to the Sentinel-1 SAR scene covering AKA (2020/5 — 2021/7), and obtained the deformation rate distribution in the AKA area, and its deformation rate along the LOS direction is shown in Figure. 6

The results in Figure 6 show that the maximum deformation rate of Ankang expansive soil airport during the 14 months after the completion of construction is less than -45 mm/year, and the maximum deformation rate inside the airport is between -21 mm/year and -33 mm/year. Basically stable. Three large deformation areas I, II and III are identified in the monitoring area, and these three areas belong to the expansive soil fill slope area around the airport. The maximum deformation rate occurs at point P1 on expansive soil slope III on the east side of the airport, which is -44.1 mm/year. Areas I and II belong to the expansive soil slopes on both sides of the airport runway, and large deformations have also occurred in these two areas. The maximum deformation rate is between -33 mm/year and -45 mm/year.

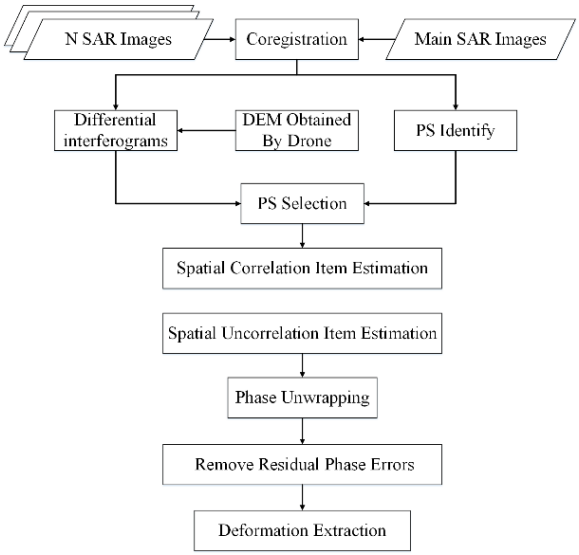

Figure 5. Flowchart of data processing.

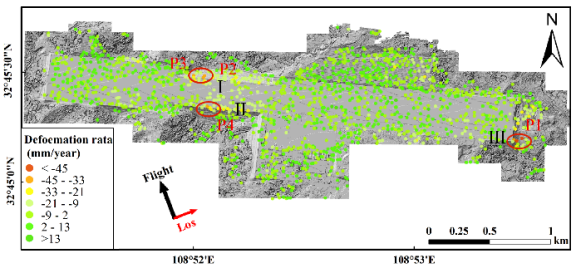

Figure 6. Spatial deformation velocity map of Ankang Airport.

In order to analyze the stability of different functional areas of Ankang Airport, we divided Ankang Airport into terminal area, runway and fill slope area, and extracted characteristic point deformation time series in the three areas for analysis.

A. *Terminal area and runway stability analysis*

As shown in Figure 5, InSAR technology successfully identified three obvious deformation areas in the fill slope area of Ankang Airport. The fill slope area is distributed around the airport flight area, all of which belong to the high fill area. The maximum fill depth reaches about 50 m. During the construction process, protective measures such as concrete pouring and

construction of anti-skid retaining walls were carried out. However, since the foundation and filling soil were mainly composed of expansive soil, the deformation in this area showed characteristics related to rainfall. Therefore, in order to analyze the relationship between the regional deformation law and rainfall of expansive soil filled slopes, the deformation time series of characteristic points (P1-P4 in Figure 5) were extracted in the I, II, and III deformation regions respectively, and the regional rainfall data such as shown in Figure 7.

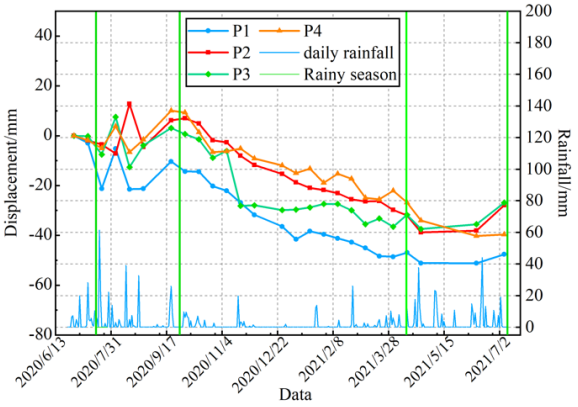

Figure 7. Time series deformation of point position in terminal area.

The Ankang area is in a subtropical monsoon climate. As can be seen from the regional rainfall information in Figure 7, the rainfall is concentrated from June to August. Therefore, we combined the local climate data to mark two more obvious rainy seasons during the monitoring period.

As shown in the P1-P4 deformation time series in Figure 7, the maximum deformation value along the LOS direction is -52.3 mm, the overall deformation interval is distributed between 15 mm and -55 mm, and the maximum accumulated deformation value at P1 is -46.7mm. The deformation trends of the characteristic points of the three filled deformation areas are similar and have certain regularity: the deformation rate gradually slows down in the rainy season, and even rebounds in the abundant rainfall environment, while the deformation trend in the non-rainy season shows the displacement along the LOS direction.

Combined with the time series deformation distribution and precipitation analysis of characteristic points in the expansive soil filling area, we believe that from June to August in Ankang, the rainfall increased, and the hydraulic properties of the expansive soil of Ankang Airport due to water absorption and expansion compensated for the post-construction deformation of the airport surface. Small deformation caused by factors such as soil consolidation and compression. This phenomenon is consistent with the expansion-shrinkage deformation characteristics of expansive soils in relation to soil moisture.

B. *Terminal area and runway stability analysis*

It can be seen from Figure 6 that the terminal area and runway of Ankang Airport are basically stable, the deformation rate is small, and the deformation points are all below -33 mm/year. According to the distribution of excavation and filling in Figure 1b, the runway and terminal area of Ankang Airport were subjected to excavation and excavation, and feature points were extracted for time series deformation analysis, as shown in Figure 8.

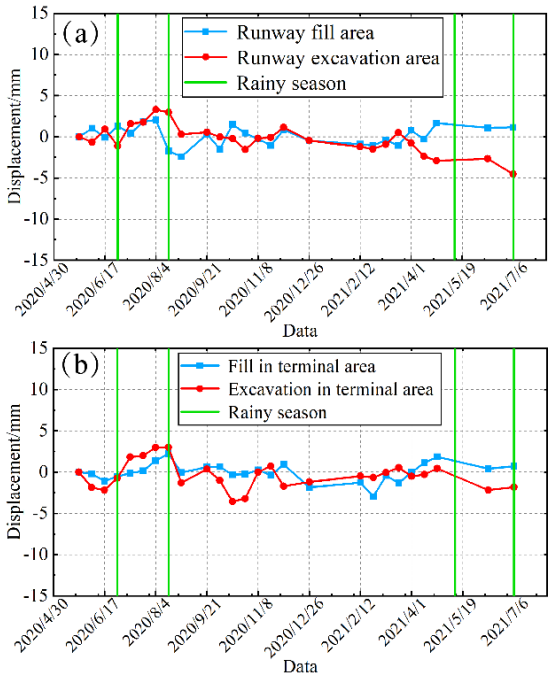

Figure 8. Deformation diagram of the point position of the runway and terminal are.

Figure 8a shows the deformation time series of the feature points in the area with the maximum depth of the excavation and filling layers of the airport runway. From the time series deformation information of the points, it can be clearly seen that the ground rebound in a small range occurs in the runway fill area during the wet season, and the maximum deformation value is 3.6 mm. Between ±5 mm, this deformation interval belongs to the normal post-construction settlement range, the runway deformation trend is stable, and the overall stability is sufficient to meet the functional requirements such as navigation.

Figure 8b shows the deformation time series of the feature points in the area with the maximum depth of excavation and filling layers in the airport terminal area. From the point time series deformation information, it can be seen that the deformation trend of the airport plane (station) flat area and the runway filling area is similar. The elastic phenomenon, the maximum deformation amount reaches 3.6 mm, and the cumulative deformation amount is small, which is -2 mm, which is basically in a stable state; the time series deformation information of the points in the excavation area within the machine (station) flat can be

seen that the point has continuous deformation, and the cumulative deformation Variable less than -4 mm. The overall deformation of the machine (station) flat area is small, and the deformation is distributed between ±4 mm and tends to be stable.

C. *Filled area deformation analysis*

In general, the consolidation settlement of the foundation under the fill, the post-construction settlement caused by the self-compression of the fill part, and the uneven settlement caused by the discontinuous construction are the main reasons for the deformation of high-fill buildings. The original terrain of Ankang Airport is a mountainous area with large undulating terrain, so Ankang Airport has carried out intense excavation and filling construction. According to the collected engineering data, the distribution of excavation and filling is shown in Figure 9.

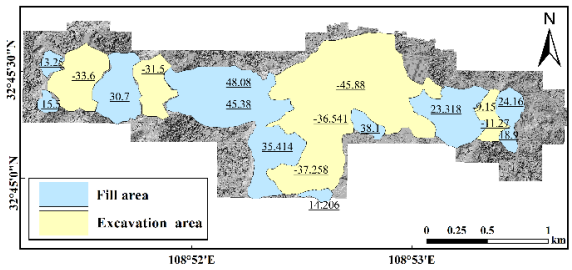

Figure 9. Ankang Airport excavation and filling distribution map.

As shown in Figure 9, the maximum fill thickness of Ankang Airport is over 48 m, the maximum excavation depth is over 45 m. The excavation and fill areas are staggered, and the fill is over 30,000,000 m^3. In order to analyze the relationship between Ankang expansive soil airport fill and surface deformation, we combined the construction distribution of excavation and filling with the InSAR deformation monitoring results shown in Figure 5. The deformation rate of the monitoring points in the study area and the depth of the filling volume where they are located are extracted for analysis, as shown in Figure 10.

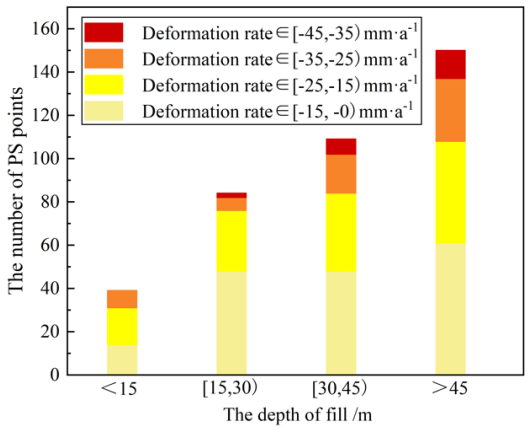

Figure 10. Relationship between deformation rate and filling depth.

It can be seen from Figure 10 that with the increase of the thickness of the fill body, the number of settlement observation points and the deformation rate increase significantly, and the distribution and thickness of the fill soil obviously affect the distribution and size of the surface deformation. The areas with the most obvious deformation are all distributed in the area where the depth of the fill layer is greater than 30 m, and the deformation monitoring points in this area account for 70% of all the monitoring points of deformation and settlement. The monitoring points with velocity >-35 mm/year, and the larger deformation points with deformation rate >-25 mm/year are concentrated in the area with layer depth > 45 m. On the contrary, in the area of fill layer depth < 15 m, the number of settlement points is less and the deformation rate value is smaller. This shows that the compressive deformation of the fill soil at different depths and the pressure on the undisturbed soil below increase with the depth of the fill layer. Therefore, the compressive deformation of the fill soil of Ankang Airport is an important cause of surface deformation.

From the analysis in this chapter, it can be seen that the main factors affecting the deformation law of Ankang Airport can be summarized as follows:

1) Combining the data of excavation and filling, it is found that the degree of deformation has a strong correlation with the depth of filling;
2) The deformation trend of the filling area is similar, and there are different degrees of rebound phenomenon in the rainy season;
3) The change of the deformation trend of Ankang Airport There is a strong correlation with regional precipitation.

V. Conclusions

To meet the local economic development and improve the regional aviation network, Ankang Airport was built in the expansive soil area after a huge filling project. However, due to the expansion and contraction characteristics of expansive soils and the weakness of fill soil foundations, Ankang Airport faces adverse environmental impacts. At present, the airport has been fully put into use, therefore, the stability of the airport area is a matter of public concern.

We have retrieved for the first time the deformation history and rate of the Ankang Airport platform using data from SAR sensors and drone sensor. The results from MT-InSAR have demonstrated that the Ankang Airport platform has experienced heterogeneous ground deformation Since the airport was put into use.

A total of 26 ascending Sentinel-1 images were used, which were acquired from May 2020 to July 2021. The pattern and spatiotemporal evolution characteristics of the surface deformation of Ankang Airport after main construction were fully Completed, providing important deformation information on Xiamen New Airport. The research results have important guiding

significance for airport stability rating, safe operation and unstable area governance. In addition, the special dilatation-contraction deformation characteristics that are closely related to expansive soil and rainfall have also been successfully verified. The main conclusions that can be drawn are as follows:

1) From May 2020 to July 2021, a total of three main deformation areas were identified in the Ankang Airport area, all of which belong to expansive soil fill slopes. The instability of expansive soil slope is the main geological disaster facing Ankang Airport at present.
2) The relationship between deformation rate and filling depth, as well as the relationship between deformation time series and rainfall, indicate that the surface deformation of the Ankang expansive soil airport is caused by the combined action of the consolidation and compression of the filling soil and the expansion and shrinkage characteristics of the expansive soil.
3) The Ankang Airport runway and the terminal area have small ground deformation variables, and the overall stability meets the design requirements and can meet the official operation needs of the airport.

In general, the monitoring results of the time-series InSAR monitoring technology based on elevation correction in the Ankang airport area show that the deformation law of the airport area is highly consistent with the expansion and contraction characteristics of expansive soil. Although the airport has not experienced significant surface deformation for the time being, its temporal deformation trend related to precipitation shows that long-term deformation monitoring of Ankang expansive soil airport is very necessary after the airport starts operation, and related research needs a shorter revisit period The SAR data and soil moisture data can be used for longer-term deformation monitoring and mechanism analysis.

VI. Acknowledgements

Project supported by the National Key Research and Development Program of China (2019YFC1509802).

Projects supported by the National Science Foundation of China (42074041;41731066).

Projects supported by the Open Fund of the State Key Laboratory of Geo-Information Engineering (SKLGIE2019-Z-2-1).

References

Berardino, P., Fornaro, G., and Lanari, R. (2002). A New Algorithm for Surface Deformation Monitoring Based on Small Baseline Differential SAR Interferograms. *IEEE Transactions on Geoscience and Remote Sensing*, Vol 40, No.11, pp. 2375-2383.

Fattahi, H., and Amelung, F. (2013). DEM Error Correction in InSAR Time Series [J]. *IEEE Transactions on Geoscience and Remote Sensing*, Vol 51, No.7, pp. 4249-4259.

Ferretti, A., Prati, C., and Rocca, F. (2001). Permanent Scatterers in SAR Interferometry. *IEEE Transactions on Geoscience and Remote Sensing*, Vol 39, No.1.

Gabriel, A.K., Goldstein, R.M., and Zebker, H.A. (1989). Mapping Small Elevation Changes over Large Areas: Differential Radar Interferometry. *Journal of Geophysical Research Solid Earth*, Vol 94, pp. 9183-9191.

Hooper, A., Zebker, H., Segall, P. and Kampes, B. (2004). A new method for measuring deformation on volcanoes and other natural terrains using InSAR persistent scatterers. *Geophysical Research Letters*, 31, No 23, pp. 1-5.

Jiang, Y., Liao, M., and Wang, H. (2016). Deformation Monitoring and Analysis of the Geological Environment of Pudong International Airport with Persistent Scatterer SAR Interferometry. *Remote Sensing*, 8, No 12, pp. 1021.

Jiang, L., and Lin, H. (2010). Integrated Analysis of SAR Interferometric and Geological Data for Investigating Long-Term Reclamation Settlement of Chek Lap Kok Airport, Hong Kong. *Engineering Geology*, 110, pp. 77-92.

Liu, X., Zhao, C., and Zhang, Q. (2019). Characterizing and Monitoring Ground Settlement of Marine Reclamation Land of Xiamen New Airport, China with Sentinel-1 SAR Datasets. *Remote Sensing*, 11, No 5, pp. 585.

Short, N., Leblanc, A.M., Laden, W., Olden Borger, G., Mathon-Dufour, V., and Brisco, B. (2014). Radarsat-2 d-insar for ground displacement in permafrost terrain, validation from Iqaluit Airport, Baffin Island, Canada. *Remote Sensing of Environment*, 141, pp. 40-51.

Touzi, R., and Lopes, A. (1999). Bruniquel J, et al. Coherence estimation for SAR imagery. *IEEE Transactions on Geoscience and Remote Sensing*, 37, No 1, pp. 135-149.

Wu, Q., Jia, C., Chen, S., and Li, H. (2019). SBAS-InSAR Based Deformation Detection of Urban Land, created from Mega-Scale Mountain Excavating and Valley Filling in the Loess Plateau: The Case Study of Yan'an City. *Remote Sensing*, 11, No. 14, pp. 1673.

Wu, S., Yang, Z., and Ding, X. (2020). Two Decades of Settlement of Hong Kong International Airport Measured with Multi-temporal InSAR [J]. *Remote Sensing of Environment*, 24, No 8, pp. 111976.

Zhuo, G., Dai, K., and Huang, H. (2020). Evaluating Potential Ground Subsidence Geo-Hazard of Xiamen Xiang'an New Airport on Reclaimed Land by SAR Interferometry. *Sustainability*, 12, pp. 6991.